DOI: 10.1002/stco.202000058

Johan Maljaars, Thomas Misiek

ARTICLE

Fatigue resistance of steel ropes: failure criterion

Background to the verification in prEN 1993-1-11:2020

Many steel rope systems are subjected to fluctuating tensile loads and therefore can fail due to fatigue. Available fatigue test data indicate that rope diameter, mean stress, socket type, lay angle and rope length influence the fatigue resistance. Most of the tests were terminated before full failure of the ropes. This paper shows that the test termination criterion, such as fracture of the first wire, fracture of 5 % of the wires or full rope fracture, has a large influence on the resulting fatigue resistance. A probabilistic analysis is carried out for a rope system in a bridge, demonstrating that the required structural reliability levels are met when considering full failure as the end-of-life criterion for ropes.

Keywords rope systems; fatigue tests; strand; probabilistic analysis; structural reliability; Eurocode 3

1 Introduction

Steel ropes are often used for spanning large distances in engineering structures such as bridges, long-span roofs and lifts. Various types of rope are available, see Fig. 1. The design of ropes and their applications and anchorage systems in actual structures are based on long-term practical experience, where lessons learned from earlier days have been incorporated. The European standard EN 1993-1-11 [1] provides verification rules for the structural design of ropes. One of the verifications concerns the fatigue life. A Wöhler or S-N curve is provided for this, which gives the 95 % exceedance fraction of the number of cycles to failure N (abscissa) as a function of the applied stress range $\Delta\sigma$ (ordinate), with the latter defined as the load range divided by the metal area of the rope cross-section.

During the revision process of the standard [2], concerns were raised regarding the correctness of the S-N curve, and an alternative curve was suggested, see [3], [4]. Fig. 2 shows the two curves, which are both defined by

$$\log_{10}\left(N\right)=\begin{cases}\log_{10}\left(N^*\right)+m_1\log_{10}\left(\Delta\sigma^*\right)- \\ m_1\log_{10}\left(\Delta\sigma\right) & \text{if } \Delta\sigma\geq\Delta\sigma^* \\ \log_{10}\left(N^*\right)+m_2\log_{10}\left(\Delta\sigma^*\right)- \\ m_2\log_{10}\left(\Delta\sigma\right) & \text{if } \Delta\sigma<\Delta\sigma^*\end{cases} \quad (1)$$

where N^* is the number of cycles at the knee-point of the curve, $\Delta\sigma^*$ is the corresponding stress range and m_1 and m_2 are the inverse reciprocal slopes of the two branches of the curve (see Fig. 2 for the values). The first branch of the curve, with parameter m_1, is deduced from constant-amplitude fatigue tests and the second branch is an extension of that curve accounting for the effect of variable amplitude load.

The background to the S-N curve in [1] is lacking, but it is likely that the curve is based on evaluation of test data by Chaplin [5], given the agreement with S-N curves. The S-N curve in [5] is based on fatigue tests carried out up to full failure of the rope. The alternative S-N curve in Fig. 2 is introduced in [3], based on information from [6] and [7]. It is derived from the suitability tests required for rope systems. A suitability test comprises a fatigue test carried out for a certain endurance followed by a tensile test up to fracture of the rope [8]. Similarly to the design of ropes, the suitability test condition and criterion are based on long-term experience. Using data from suitability tests and assuming slope parameters equal to those of welded joints in [9] – thus implicitly (and conservatively) assuming that the fatigue life initiation period is limited – allowed the alternative S-N curve to be derived.

It is evident from Fig. 2 that the difference between the two curves is especially large at relatively low stress ranges and large numbers of cycles; however, this part is relevant

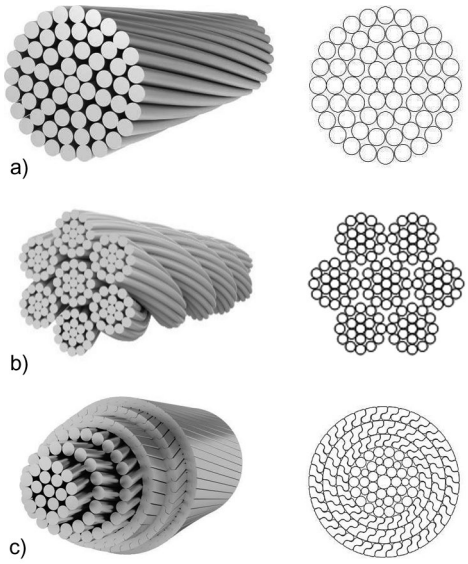

Fig. 1 Rope assemblies (3D figures published by courtesy of Fatzer AG): a) spiral strand rope, b) stranded rope, and c) full-locked coil rope

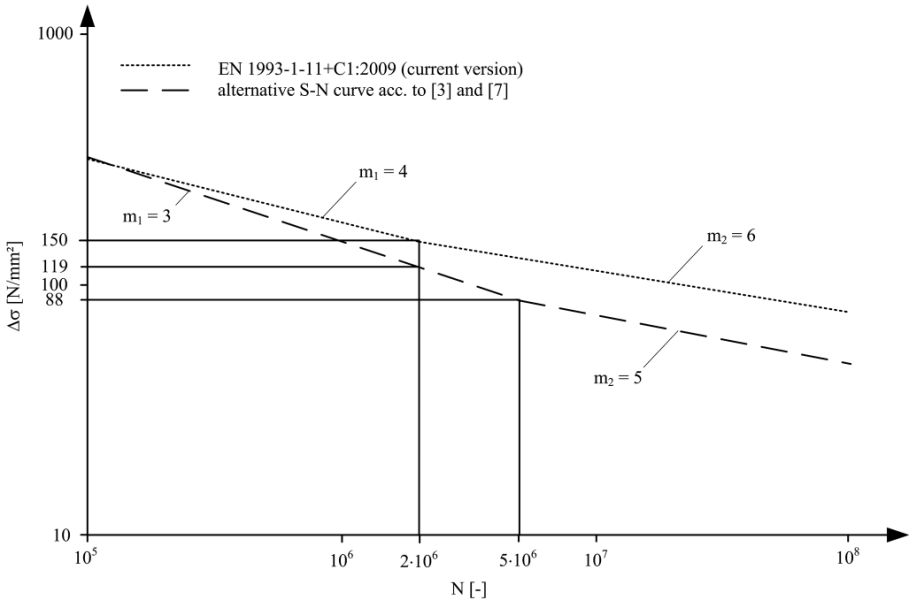

Fig. 2 S-N curve for ropes in [1] and alternative curve in [3]

for many practical applications. For this reason, fatigue tests carried out in the past are re-evaluated in section 2. It appears that the differences in fatigue resistance reported by different authors are partly due to the different failure criterion adopted, such as failure of the first wire, failure of 5 % of the wires, or full rope failure. Section 3 describes a probabilistic assessment for determining which of these criteria satisfies the required reliability. This paper is closely connected with an accompanying paper [10] in which the S-N curve is derived from tests on full-locked coil ropes. The two papers provide the background to the fatigue resistance of ropes for the upcoming revision of EN 1993-1-11 [2].

2 Evaluation of fatigue tests on ropes

In the past, tests have been carried out on rope systems and on the individual wires used to construct ropes. The fatigue resistance of individual wires appears to be significantly higher than that of rope systems [4]. The main reason for this is that fatigue failure of wires in a rope is related to fretting corrosion at the contact location of crossing wires ('trellis points') [11], [12]. The severity of fretting corrosion is related to the combination of pressure and relative displacement between the wires [13], [14], which causes high temperatures, resulting in galling and oxidation [15], and a microcrack can develop at this location. Another reason for the inferior performance of strands is related to the quality of the production process, which determines the variability in stress level between the individual wires of a strand [16]. Hence, test data should be collected from rope systems and not from individual wires.

Large test databases have been collected and evaluated for spiral strand ropes and stranded ropes. Various works by Chaplin, e.g. [5], [16], [17], are of particular importance because of the consistent evaluation of many test data. The scatter in the fatigue resistance appears very substantial if all data are jointly evaluated and it is much larger than the scatter of individual test series. Sources of scatter are geometrical and quality differences between strands and types of socket, but also differences between test conditions such as frequency. Overviews of the S-N curves resulting from the collection of large databases are given in [18] and [19]. The S-N curve is expressed in [18] with the range as a fraction of either the actual breaking force (in the past referred to as ultimate breaking load, UBL) or the calculated minimum breaking force $F_{c,min}$ considering the spinning loss factor (in the past referred to as minimum breaking load, MBL) and in [19] as an equivalent load amplitude, in line with the custom in the UK and the USA, and Germany, respectively.

A significant influence of the strand diameter on the fatigue resistance was observed in [20] for ropes in a diameter range 4 mm ≤ D ≤ 36 mm. The fatigue life was found to decrease by a factor of 1.7 or 2.7 in the case of stranded ropes and spiral strand ropes respectively for a diameter increasing by a factor of 2. A similar factor of 2 to 3 applied to the fatigue life for a two times larger diameter range is mentioned in various papers by Raoof, e.g. [12], based on a theoretical model of fatigue fretting in strands. Adding data from [21], Feyrer [19] extended the findings in [20] to rope diameters 4 mm ≤ D ≤ 127 mm by also accounting for the difference in number of wires per rope. However, Chaplin [16] concluded that the S-N curves of small diameter ropes are flatter – i.e. the fatigue life is more sensitive to a variation in load range – than those of large diameter ropes and that the S-N curves of different diameter systems cross each other, i.e. small diameter ropes perform better at low stress ranges (long endurance) but worse at high stress ranges (short endurance) compared with large diameter ropes. He attributes the difference to different processing, where small diameter

wires (used in small diameter ropes) require additional heat treatment and have different residual stresses across the wire. Another potential cause, not mentioned in the literature, is the temperature generated during testing due to the fretting mechanism. A high temperature is detrimental to fatigue performance, and so specimens are therefore often cooled from the outside during testing. Cooled or not, the core of a large diameter rope is expected to be hotter than that of a small diameter rope, and the effect may be more pronounced in the high-frequency testing that is especially applied at low stress range levels and high endurances.

Another influencing factor is the mean load of the cycle. The fatigue resistance of individual wires reduces with increasing mean load [22], but spiral strand ropes and stranded ropes exhibit a different behaviour. The endurance is observed to be highest at a moderate minimum load level and lower at a high, but also nearly zero, minimum load [19], [20], [23]. This might be due to the variation in stress per wire. This variation is larger at low stress levels due to the lay quality and the absence of early yielding of the most highly stressed wires [16].

Based on a theoretical model describing the fretting mechanism in ropes, Raoof [24] concluded that the lay angle of the wires in the strands is an important factor affecting the fatigue performance. However, the lay angle in most rope systems does not vary to a great extent. It is usually in the order of 16° to 18° for the outer layers, with some exceptions of 15° or 19°. Except for Raoof's work, the lay angle is not usually considered in the statistical evaluation of fatigue test data for ropes.

Finally, the rope length is of importance. The test length should include at least one recovery length or 10 lay lengths [24], or be at least 5 m [2]. Wire fractures are often observed near the sockets in tests. However, tested lengths are often much shorter than the rope lengths used in real structures. From a statistical point of view, it can be expected that the probability of failure somewhere in the free length of a long rope, i.e. a series system consisting of multiple recovery lengths, exceeds that of the socket regions if the rope length exceeds a certain value. A statistical model considering the length effect based on a Weibull distribution is given in [25]. The effect may be obtained from tests on small diameter ropes as these can be tested at relatively large length-to-diameter ratios. Esslinger [26] tested 0.6 inch diameter spiral strand ropes with lengths of 1040, 2030 and 10430 mm (data in [19]). The data show some indications that the transition from finite life to nearly infinite life reduces with the length. Excluding the data in the transition region, the endurance of the longest wires was approx. 1.5 times shorter than the other two lengths for an equal failure probability.

Applying linear regression to the test data and using the S-N curve model of Eq. (1), Chaplin [16] provides a slope variable $m_1 = 4$ to $m_1 = 9$ for large and small diameter ropes respectively for individual test series on a single geometry. Values close to $m_1 = 4$ are also given in [18] for individual series involving larger diameter ropes. Owing to the statistical nature of the regression, a large scatter reduces the value of the slope parameter because the model is less able to describe the data properly. This is the reason why the slope parameter reduces if multiple test series, containing multiple geometries, are combined in the regression. A slope parameter $m_1 = 3.44$ is suggested in [18] when combining all data. The load range at a mean number of cycles of $2 \cdot 10^6$ is 16 % of the MBL for both spiral strand ropes and stranded ropes according to that same source (263 and 109 test data respectively), where run-outs were considered as failures. The characteristic fatigue resistance – defined in [18] as associated with the mean minus two standard deviations of the fatigue life equal to $2 \cdot 10^6$ cycles – is approx. 8.5 % of $F_{c,min}$ according to the same source.

Three regressions of fatigue tests on relatively large diameter ropes are used in a comparison later in this paper:

- Chaplin [17] analysed data in Casey [21] covering 40, 70 and 127 mm diameter ropes with a lay angle of 18°. The failure criterion adopted was the number of cycles to complete failure of the rope. Fig. 3 provides a selection of the test results. The proposed characteristic S-N curve (1st branch) is

$$\log_{10} N = \log_{10}\left(3.75 \cdot 10^{10}\right) - 4 \log_{10}\left(\Delta p'\right) \tag{2}$$

  where $\Delta p'$ is the load range as a fraction of UBL minus minimum load.
- Tilly [27] tested 35, 44, 53 and 63 mm diameter spiral strand ropes and stranded ropes with lay angles of 14°, 18° and 21°, see Fig. 4. Again, test data across the two types of rope did not differ significantly and they were treated as one population. The failure criterion adopted was the number of cycles to the first five visibly fractured wires. The characteristic S-N curve in Tilly is defined as giving the 95 % lower bound fatigue life:

$$\log_{10} N = \log_{10}\left(2 \cdot 10^9\right) - 3.3 \log_{10}\left(\Delta p\right) \tag{3}$$

  where Δp is the load range as a fraction of $F_{c,min}$. Fig. 4 shows only one test failing at a relatively low load level of approx. 10 % of $F_{c,min}$. Had this test been treated as an outlier and therefore ignored in the regression, a shallower S-N curve would have resulted. The number of cycles between the 1st and the 5th broken wires was between 0.5 and 2 times the number of cycles to the 1st broken wire.
- Raoof [11] developed a theoretical prediction model for first wire fracture. He compared his model with tests in [12], [17], [24], [27], see Fig. 5. He explicitly accounts for the lay angle and distinguishes between failures in the free length or near the sockets. Tab. 1 provides the proposed slope parameter and the characteristic fatigue resistance to 1st wire fracture at $2 \cdot 10^6$ cycles for 127 mm diameter ropes.

Tab. 1 Fatigue resistance (1st wire fracture) of spiral strands in air according to the theoretical model of Raoof [12]

Location	Lay angle	Δp	m_1
Free length	12°	0.088	2.4
	18°	0.064	2.1
	24°	0.049	1.9
Socket region	12°	0.054	1.8
	18°	0.039	1.6
	24°	0.030	1.5

These three sources give significantly different fatigue resistance values.

The construction of full-locked coil ropes is different from that of spiral strand ropes and stranded ropes, and this can affect the fatigue resistance. As most data on full-locked coil ropes is drawn from German sources, the fatigue resistance is expressed in terms of stress range, with the latter defined as the applied load range divided by the metal area. Sedlacek et al. [6] and Paschen [7] collected test data from suitability tests on full-locked coil ropes from various sources, all tested with a stress range of 150 N/mm^2, terminated at $2 \cdot 10^6$ cycles and thereafter subjected to a static tensile test up to full rope failure. They developed further an empirical prediction model initially proposed by Saul and Andrä [28] which determines the relative loss of resistance as a function of the number of fractured wires. Based on this model, the 95 % fraction of the relative loss in rope resistance δ was derived in [6] and [7] as a function of the stress range at a life of $2 \cdot 10^6$ cycles $\Delta\sigma_C$, see the black line in Fig. 6.

As a comparison, Fig. 6 also shows the characteristic fatigue resistance values of large diameter spiral strand ropes and stranded ropes mentioned in the previous section. The calculated breaking force considered in this comparison – expressing the S-N curves of Eqs. (2) and (3) and Tab. 1 in terms of stress range – is the metal area multiplied by the nominal tensile strength of the wires f_{uk}, and ignores the spinning loss factor for reasons of simplicity. A value f_{uk} = 1 500 N/mm^2 is considered to be a reasonable strength value for full-locked coil ropes. Fig. 6 shows that the trend in the fraction of rope fractures versus the characteristic fatigue resistance is consistent across the different studies. Moreover, despite the differ-

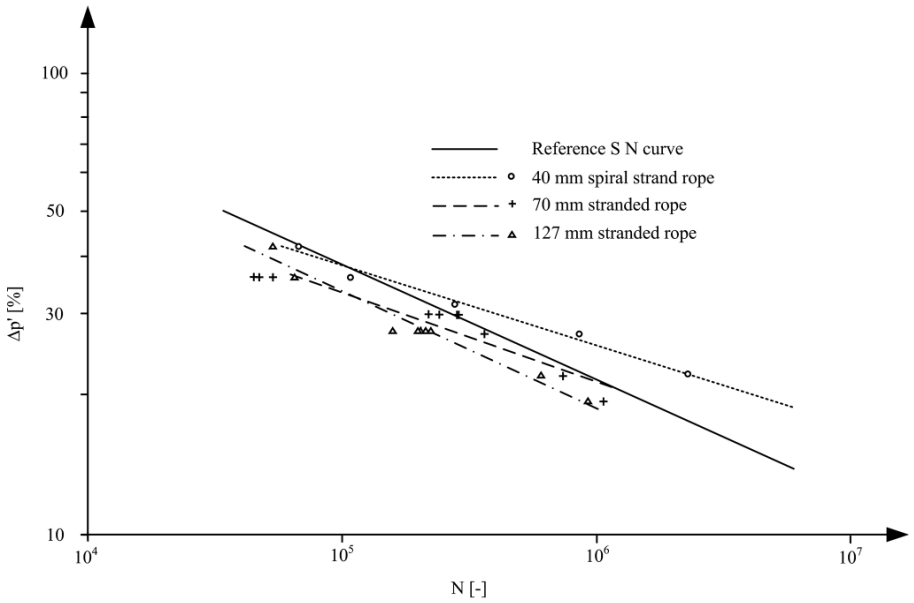

Fig. 3 Selection of test data evaluated by Chaplin [17]

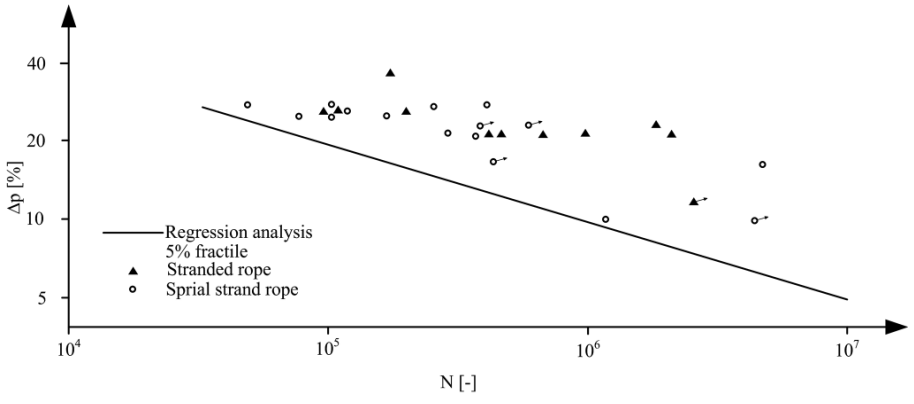

Fig. 4 Test data from Tilly [27]

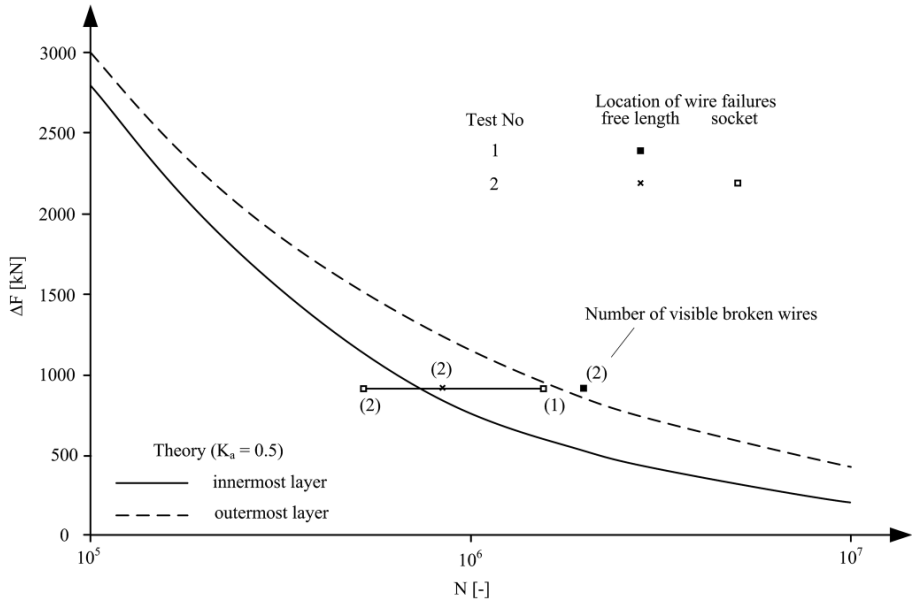

Fig. 5 Selection of test data by Raoof [12], [24] for 1st wire failure in a 102 mm diameter strand rope with 17° lay angle

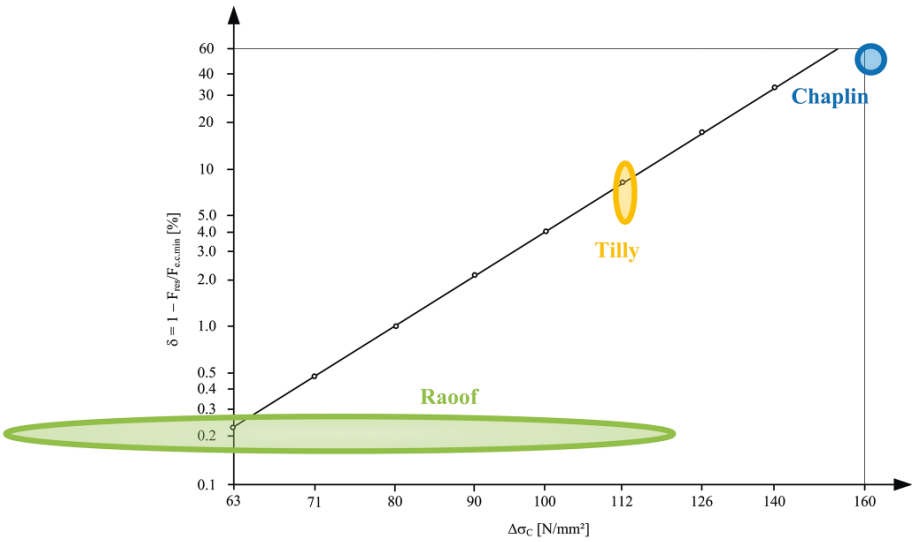

Fig. 6 Relation between the characteristic fatigue resistance (at 2 million cycles) and the relative loss of resistance according to Sedlacek et al. [6] and Paschen [7] (black line) and comparison with the resistance values of Raoof [11], Tilly [27] and Chaplin [17]

ence in rope construction, the results, even quantitatively, are in reasonable agreement. Fig. 6 indicates that the fatigue resistance is highly dependent on the termination criterion of the test.

3 Probabilistic analysis for evaluating end-of-test criterion

As the termination criterion appears to be so important for the fatigue resistance, the question is: Which termination criterion should be selected for the fatigue design in the standard EN 1993-1-11 [2]? This section describes a probabilistic assessment where the structural reliability of a design based on full failure of the rope is compared with the target reliability as put forward in Eurocode EN 1990 [29].

3.1 Target reliability

The Eurocodes allow a structure to be assessed with a 'safe-life concept', for which no inspections are foreseen or considered at the design stage, and a 'damage-tolerant concept', which requires periodic visual inspections. Applying a safe-life concept, it is evident that the reliability at full failure of the rope should meet the reliability requirement for the ultimate limit state. Differently from, for example, welded joints, a significant warning effect (fracture of individual wires) is to be expected for rope systems. Theoretical models such as that of Raoof [11] indicate that the inner wires are subjected to the largest stress ranges in a bent strand. Tests show, however, that the wires of the outer layers usually break first. For this reason, regular visual inspections will in most cases suffice in a damage-tolerant concept, where the rope system is replaced in time.

The reliability index β is defined as

$$\beta = -\Phi^{-1}\left(P_f\right) \tag{4}$$

where P_f is the probability of failure and $\Phi(\cdot)$ is the cumulative distribution function of the standard normal distribution. EN 1990 [29] provides the target reliability indices related to fatigue for a reference period of 50 years and a structure in reliability class 2. The index range $1.5 \leq \beta \leq 3.8$ depends on the inspection and repair possibilities and the tolerance to damage. The upper bound value of 3.8 corresponds to the target reliability for the ultimate limit state, and this should be met using the safe-life concept. Most ropes can be inspected and replaced (although possibly expensive and disruptive) and have a high tolerance to damage. Therefore, it is reasonable to select a reliability index closer to the lower bound value of 1.5 for the damage-tolerant concept. Bridges are usually designed for a life of 100 years, but target reliability levels are not provided for this period. The 50-year target reliability levels are therefore used conservatively for a 100-year life. Bridges are usually classified in reliability class 2 or 3. For reliability class 3, the upper bound target value for the 50-year reliability index should be increased from 3.8 to 4.3 (safe-life concept). It is unclear as to by what extent the lower bound value needs to be increased (damage-tolerant concept).

3.2 Design of the rope

A rope in a motorway bridge is considered here. As a simplification, the influence line is assumed to be that of a simply supported beam with a span of 100 m. Two cases are considered: In case 1 the rope is loaded by one slow lane only. In case 2 the rope is loaded by a slow lane and an adjacent fast lane (with overtaking trucks) and the two lanes have the same influence line (i.e. same load effect for load on the fast lane as on the slow lane). The structure is designed with Fatigue Load Model 4 (FLM4) according to EN 1991-2 and an S-N curve derived as the 95 % lower bound for full rope failure of full-locked coil ropes in the accompanying paper [10]. This S-N curve has the following characteristics: $\Delta\sigma^* = 115$ MPa, $N^* = 5 \cdot 10^6$, $m_1 = 4$ and $m_2 = 6$. The rope is designed with the cumulative damage accumulation rule of Palmgren-Miner such that the damage D_{des} according to the design procedure is equal to 1:

$$D_{des} = \sum_i \frac{n_i}{N_i} = 1 \tag{5}$$

where n_i is the number of trucks of a certain type in FLM4, each producing a stress range $\Delta\sigma_i$, and N_i is determined with Eq. (1), where $\Delta\sigma^*$ is divided by either $\gamma_{Mf} = 1.35$ for a safe-life design or $\gamma_{Mf} = 1.15$ for a damage-tolerant design.

The frequent traffic load effect is considered through Load Model 1 of EN 1991-2. The stress caused by the permanent load σ_p is tuned such that the frequent load combination effect is $0.45 f_{uk}$, which is the condition of validity of the S-N curve. This tuning procedure gives $\sigma_p = 563$ MPa for $f_{uk} = 1500$ MPa.

3.3 Reliability analysis

The designed rope is subsequently considered in a probabilistic analysis. The actual load and resistance are considered as realistically as possible in this analysis and include any uncertainties. In this case, instead of FLM4, the rope is loaded with all the vehicles in a weigh-in-motion (WIM) database recorded in the period between 1 January and 31 October 2015 on motorway A16 in The Netherlands. The WIM database contains dynamically measured axle loads, axle distances and distances between vehicles, and it is described and validated in [30]. The axle loads appear to be representative, but the number of vehicles is relatively large compared with other European motorways. It therefore forms an upper bound.

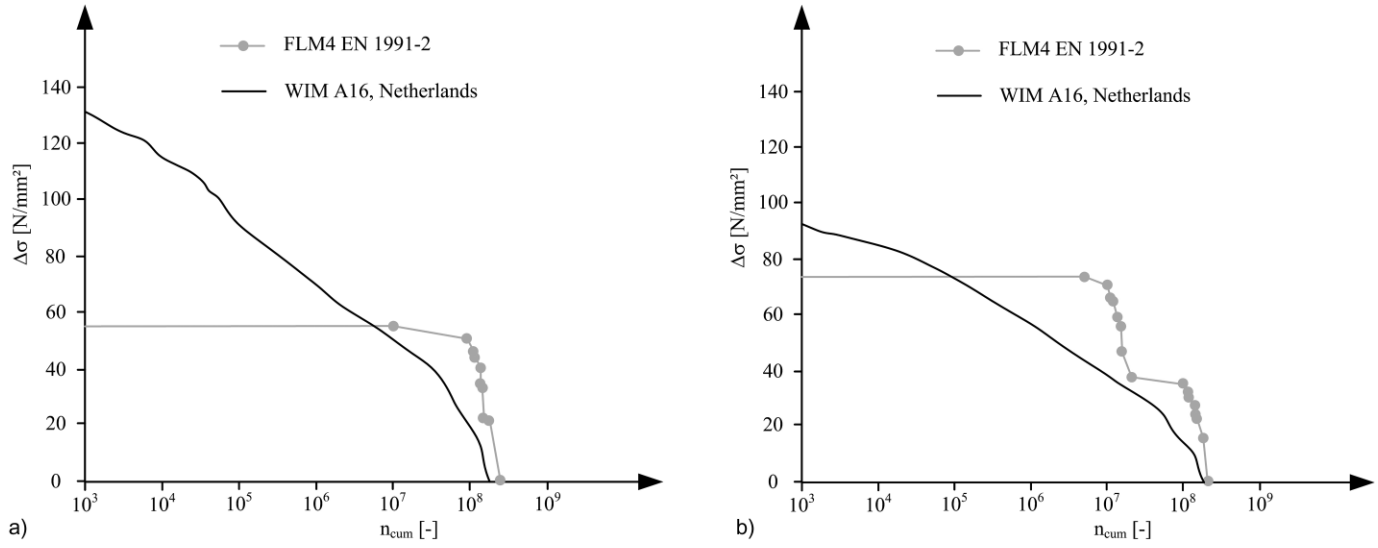

Fig. 7 Stress range versus cumulative number of cycles n_{cum} for a simply supported beam of 100 m span designed with $\gamma_{Mf} = 1.35$: a) slow lane only, b) slow and fast lanes

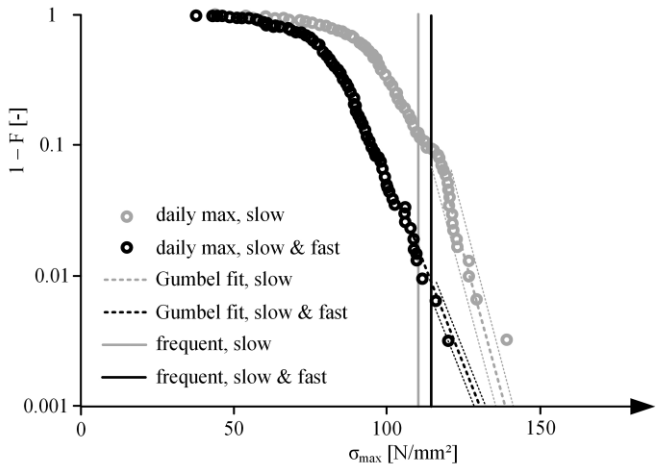

Fig. 8 Exceedance probability for maximum stress per day due to traffic load σ_{max}

All recorded axles, including the distances between them, are applied to the influence line in a specially developed software and the stress history is recorded. A rainflow counting procedure is applied, resulting in the stress range histograms. Fig. 7 provides the stress range histograms for 100 years of the designed rope using the WIM database and using FLM4 with $\gamma_{Mf} = 1.35$. The maximum stress per day due to traffic load σ_{max} is obtained from the same simulation. Fig. 8 gives this daily maximum stress a function of the exceedance fraction 1-*F*. A Gumbel distribution for *F* is used to fit the tail of the data. Fig. 8 shows its mean and mean plus or minus two standard deviations, together with the frequent values of the load effect according to EN 1991-2. Note that the stress levels are different in the two cases because to reach a damage $D_{des} = 1$ with the FLM4 model, the influence lines are different.

The number of annual heavy vehicles in the WIM database is $2.5 \cdot 10^6$. This number has remained approximately constant since the start of the measurement campaign in 2008, and measurements on other motorways show that it is approximately the maximum number that can be attained for a motorway. More traffic apparently results in more traffic jams. For this reason, a trend has not been applied to the number of vehicles.

The load effect is subject to uncertainty. The major source of uncertainty is a modelling approximation in the structural model made by the engineer. The JCSS probabilistic model code [31] provides a load effect uncertainty factor that is lognormally distributed with a mean of 1 and a standard deviation of 0.1. The load effect in terms of stress is multiplied by this model uncertainty. The stress due to life load is further multiplied by a dynamic amplification factor that takes account of dynamic interaction between the bridge and the vehicle. Measurements indicate that the dynamic amplification of main loadbearing structures is usually small. A lognormal distributed factor with a mean of 1 and a standard deviation of 0.05 is assumed here.

The damage-tolerant design concept is considered first. In practice, depending on the structure, various criteria can apply for the replacement of a rope. An (arbitrary, but not unusual) replacement criterion of 5 % of wires being fractured is applied here. The associated S-N curve is derived in [10] and its parameters are given in Tab. 2. Following the JCSS probabilistic model code [31] and DNVGL-RP-C210 [32], full correlation is assumed between the first and second branches of the S-N curve. In addition, following [31] and [32], the critical damage D_{cr} (at which failure occurs) is assumed to follow a lognormal distribution with a mean of 1 and a standard deviation of 0.3. The limit state function is

$$g\left(\boldsymbol{X},t\right) = D_{cr} - D_{n} \tag{6}$$

where $\boldsymbol{X}$ is the vector of random variables according to Tab. 2, t the time and D_n the accumulated damage using the WIM stress range histogram and the probabilistic S-N curve:

$$D_{n} = \sum_{j} \frac{1}{N_j} = 1 \tag{7}$$

where N_j is obtained with Eq. (1) for each stress range $C_{unc}C_{daf}\Delta\sigma_j$ that occurs.

The safe-life design concept will now be considered, where the probabilistic S-N curve for full rope failure is used [10]. Here, it is necessary to account for the reduc-

Tab. 2. Random variables

$\boldsymbol{X}$	Description	Distribution type	Mean	St.dev
C_{unc}	Model uncertainty	Lognormal	1.0	0.1
C_{daf}	Dynamic amplification factor	Lognormal	1.0	0.05
σ_S	Max. stress (100-year), slow lane	Gumbel	159.	6.3
	Max. stress (100-year), slow & fast lanes		161.	9.6
$\log_{10}(N^*) + m_1\log_{10}(\Delta\sigma^*)$	S-N curve, 5 % wire fractures [a]	Student's t (n = 29, ν = 27)	15.78	0.212
	S-N curve, full failure [b]		15.95	0.189
D_{cr}	Critical damage	Lognormal	1.0	0.3
f_u	Tensile strength of wires	Normal	$1.1f_{uk}$	$0.05f_{uk}$

[a] $m_1 = 4.41$, $m_2 = m_1 + 2$, $N^* = 5 \cdot 10^6$, full correlation between 1st and 2nd branch

[b] $m_1 = 4.33$, $m_2 = m_1 + 2$, $N^* = 5 \cdot 10^6$, full correlation between 1st and 2nd branch

tion in static resistance of the strand with increasing fatigue damage. The remaining static resistance σ_{res} can be described by (see [10])

$$\sigma_{res} = \begin{cases} 0.45 f_u + \\ 0.55 f_u \cdot \left(1 - \left(\frac{D_n}{D_{cr}}\right)^{b'}\right)^{\frac{1}{m_1 b' + 1}} & D_n \le D_{cr} \\ 0 & D_n > D_{cr} \end{cases} \quad (8)$$

where f_u is the actual tensile strength of the wires with an assumed distribution according to Tab. 2 and factor $b' = 2$. Assuming no dependency between days of maximum load effect, the Gumbel distribution F_T for the maximum traffic load effect in 100 years σ_s can be approximated by $F_T = F^T$, where T is the number of days in 100 years ($T = 36\,525$, F in Fig. 8). The limit state function is

$$g(\boldsymbol{X}, t) = \sigma_{res} - \sigma_s C_{unc} C_{daf} - \sigma_p C_{unc} \quad (9)$$

Thus, a conservative approximation is adopted that the maximum load effect occurs at the end of the service life, at maximum fatigue deterioration of the rope.

3.4 Results

The reliability indices for the two cases are determined using the first-order reliability method (FORM). Tab. 3 provides the results. It shows that the reliability index for a structure loaded by two (slow and fast) lanes with equal influence lines is larger than that of a structure loaded by one (slow) lane. This is related to the inability of FLM4 to represent accurately the WIM database for both situations [30]. The result is a relatively heavy structural design, related to the actual loading, for a two-lane structure compared with a one-lane structure.

All calculated reliability indices are equal to or higher than the target values. In most practical cases, ropes are loaded in a combination that is somewhere between that of two lanes with equal influence lines and that of one lane, and this gives a reliability that is significantly higher than the target value. Hence, the characteristic S-N curve derived for design purposes and evaluated for full rope failure meets the reliability requirements for the ultimate limit state in EN 1990 [29].

Tab. 3. Reliability indices calculated with FORM

γ_{Mf}	Probabilistic S-N curve	Two lanes	One lane
1.15	5 % fractures	3.3	1.9
1.35	Full rope failure	5.0	4.3

4 Conclusions

This paper has evaluated existing tension-tension fatigue test data for steel ropes. Large test databases are available for spiral strand ropes and stranded ropes. They show the following:

- The fatigue resistance of small diameter ropes is different from that of large diameter ropes: The S-N curve is flatter (i.e. is more sensitive to changes in stress range) and the fatigue resistance at $2{\cdot}10^6$ cycles is larger for small diameter ropes.
- The fatigue resistance also depends on the mean stress. A complex interaction takes place, resulting in the highest fatigue resistance being observed at a moderate mean stress level.
- Socket type, lay angle and rope length also appear to be important for the fatigue resistance.

A probabilistic analysis reveals that the S-N curve as derived for full rope failure satisfies the required reliability levels if the recommended partial factors adopted in the design are 1.35 or 1.15 for safe-life or damage-tolerant design respectively.

Acknowledgements

We would like to thank the members and experts of committee CEN TC250/SC3/WG11, responsible for developing prEN 1993-1-11, for the discussions that initiated this research. We are also grateful to Mohammed Raoof for providing additional explanations to his papers. The Dutch Road Authority, Rijkswaterstaat, is acknowledged for its financial support of this study.

References

[1] EN 1993-1-11+C1 (2009) Eurocode 3: *Design of steel structures – Part 1-11: Design of structures with tension components*. Brussels: CEN.

[2] prEN 1993-1-11 (2020) Eurocode 3: *Design of steel structures – Part 1-11: Design of structures with tension components.* 2nd draft for enquiry. Brussels: CEN.

[3] Annan, R. et al. (2017) *Design of tension components: Revision and further development of EN 1993-1-11* in: CE/papers 1, 14th Nordic Steel Construction Conf., 18–20 Sept 2019, Copenhagen, Denmark, pp. 3831–3840.

[4] Annan, R. et al. (2020) *Revision of EN 1993-1-11 – fatigue design rules for tension components* in: Steel construction 13, pp. 61–75.

[5] Chaplin, C. R.; Potts, A. E. (1991) *Wire Rope Offshore – a Critical Review of Wire Rope Endurance Research Affecting Offshore Applications*. HMSO Publication OTH 91 341.

[6] Sedlacek, G.; Lopetegui, J.; Neuenhaus, D.; Merzenich, G.; Heinemeyer, C.; Kuck, J. (1995) *Untersuchungen zum Schwingungs- und Ermüdungsverhalten der Seile und Kabel abgespannter Brücken mit Fußpunkterregung*.

RWTH Aachen, Final report for DFG research project SE 351/10-2.
[7] Paschen, M.; Dürrer, F.; Rentmeister, F. E. (2020) *Ermüdungssicherheit von vollverschlossenen Seilen mit Korrosionsschäden – BASt-Bericht B 146*. Bergisch Gladbach: Bundesanstalt für Straßenwesen, https://bast.opus.hbz-nrw.de/frontdoor/index/index/docId/2336.
[8] Technische Lieferbedingungen und Technische Prüfvorschriften für vollverschlossene Seile (2017). Bergisch-Gladbach: Bundesanstalt für Straßenwesen.
[9] prEN 1993-1-9 (2020) Eurocode 3: *Design of steel structures – Part 1-9: Fatigue.* 2nd draft for enquiry. Brussels: CEN.
[10] Maljaars, J.; Misiek, T. (2021) *S-N curve for full locked coil ropes – Background to the verification in prEN 1993-1-11:2020* in: Steel Construction (accepted for publication). https://doi.org/10.1002/stco.202100009.
[11] Raoof, M. (1996) *Axial fatigue life prediction of bridge cables* in: Harding, J. E.; Park, G. A. R.; Ryall, M. J. (eds.) *Bridge Management*, 3rd ed., London: E&FN Spon.
[12] Raoof, M.; Davies T. J. (2008) *Axial fatigue design of sheathed spiral strands in deep water applications* in: Int. J. Fatigue 30, pp. 2220–2238.
[13] Nishioka, K.; Nishimura, S.; Hirakawa, K. (1968) *Fundamental investigations of fretting fatigue. Part 1: On the relative slip amplitude of press-fitted assemblies* in: Bull. JSME 11, pp. 437–445.
[14] Guo, T.; Liu, Z.; Correi, J.; de Jesus, A. M. P. (2020) *Experimental study on fretting-fatigue of bridge cable wires* in: Int. J. Fatigue 131(2), 105321.
[15] Patzak, M.; Nürnberg, U. (1978) *Die Bedeutung der Reibkorrosion für nicht ruhend belastete Verankerungen und Verbindungen metallischer Bauteile des konstruktiven Ingenieurbaus* in: SFB 64, Mitteilungen 53/1978, Stuttgart University.
[16] Chaplin, C. R. (1995). *Prediction of the fatigue endurance of ropes subject to fluctuating tension* in: IOPEEC bulletin 70, pp. 31–40.
[17] Chaplin, C. R. (1993). *Prediction of offshore mooring ropes* in: Proc. of Round Cable Conf. on Applications of Wire Rope Endurance Research. Organisation Internationale Pour L'Etude de L'Endurance des Cables (OIPEEC), Round Table Conf., Delft, pp. 50–75.
[18] HSE (authors unknown) (1997) *Review of tension-tension fatigue performance of wire ropes*. Health & Safety Executive, Offshore Technology Report OTO 97 080.
[19] Feyrer, K. (2015) *Wire ropes – tension, endurance, reliability*. 2nd ed. Heidelberg: Springer.
[20] Klöpfer, A. (2002) *Untersuchung zur Lebensdauer von zugschwellbeanspruchten Drahtseilen*. Dissertation, Stuttgart University.
[21] Casey, N. F. (1993) *The fatigue endurance of wire ropes for mooring offshore structures* in: Proc. of Round Cable Conf. on Applications of Wire Rope Endurance Research. Organisation Internationale Pour L'Etude de L'Endurance des Cables (OIPEEC), Round Table Conf., Delft, pp. 24–49.
[22] Unterberg, H.-W. (1967) *Die Dauerfestigkeit von Seildrähten bei Biegung und Zug*. Dissertation, TH Karlsruhe.
[23] Wehking, K.-H. (1999) *Lebensdauer und Ablegereifeerkennung von Drahtseile unter Zugschwellbeanspruchung*. Stuttgart University.
[24] Raoof, M. (1997) *Effect of lay angle on various characteristics of spiral strands* in: Int. J. Offshore Polar Eng. 7, pp. 54–62.
[25] Castillo, E.; Canteli, A. F.; Esslinger, V.; Thürlimann, B. (1985) *Statistical model for fatigue analysis of wires, strands and cables* in: IABSE proc. vol. 9, pp. 1–38.
[26] Esslinger, V. (1992) Fatigue testing of wires and strands. IABSE Workshop, Madrid.
[27] Tilly, G. P. (1988). *Performance of bridge cables* in: Proc. of 1st Oleg Kerensky Memorial Conf., Institution of Structural Engineers, London, pp. 22/4–8/4.
[28] Saul, R.; Andrä, W. (1981) *Zur Berücksichtigung dynamischer Beanspruchungen bei der Bemessung von verschlossenen Seilen stählerner Straßenbrücken* in: Die Bautechnik 4, pp. 116–124.
[29] EN 1990+A1+C2. (2011) Eurocode: *Basis of structural design*. Brussels: CEN.
[30] Maljaars, J. (2020) *Evaluation of traffic load models for fatigue verification of European road bridges* in: Engng. Struct. 225(12), 111326.
[31] JCSS (2020) *Probabilistic model code, part 3: Resistance models*. Apr 2011. https://www.jcss-lc.org/jcss-probabilistic-model-code/
[32] DNVGL-RP-C210 (2015) *Probabilistic methods for planning of inspection for fatigue cracks in offshore structures*. Oslo: DNVGL.

Authors
Prof. Dr. ir. Johan Maljaars (corresponding author)
j.maljaars@tno.nl
TNO
PO Box 155
2600 AD Delft, the Netherlands
also:
Eindhoven University of Technology, The Netherlands
Tel. +31 652803581

Dr.-Ing. Thomas Misiek
thomas.misiek@breinlinger.de
Breinlinger Ingenieure
Kanalstraße 14
78532 Tuttlingen, Germany

How to Cite this Paper

Maljaars, J.; Misiek, T. (2021) *Fatigue resistance of steel ropes: failure criterion – Background to the verification in prEN 1993-1-11:2020.* Steel Construction. https://doi.org/10.1002/stco.202000058

This paper has been peer reviewed. Submitted: 10. November 2020; accepted: 2. March 2021.